fire

MDPI

Article

Anticipating Future Risks of Climate-Driven Wildfires in Boreal Forests

Shelby Corning [1,*], Andrey Krasovskiy [1], Pavel Kiparisov [1], Johanna San Pedro [1], Camila Maciel Viana [2] and Florian Kraxner [1]

[1] Agriculture Forestry and Ecosystem Services (AFE) Group, Biodiversity and Natural Resources (BNR) Program, International Institute for Applied Systems Analysis (IIASA), Schlossplatz 1, A-2361 Laxenburg, Austria; krasov@iiasa.ac.at (A.K.)
[2] Gestión Forestal Basada en Ciencia de Datos, Universidad de Valladolid (UVA), 47002 Valladolid, Spain
* Correspondence: corning@iiasa.ac.at

Abstract: Extreme forest fires have historically been a significant concern in Canada, the Russian Federation, the USA, and now pose an increasing threat in boreal Europe. This paper deals with application of the wildFire cLimate impacts and Adaptation Model (FLAM) in boreal forests. FLAM operates on a daily time step and utilizes mechanistic algorithms to quantify the impact of climate, human activities, and fuel availability on wildfire probabilities, frequencies, and burned areas. In our paper, we calibrate the model using historical remote sensing data and explore future projections of burned areas under different climate change scenarios. The study consists of the following steps: (i) analysis of the historical burned areas over 2001–2020; (ii) analysis of temperature and precipitation changes in the future projections as compared to the historical period; (iii) analysis of the future burned areas projected by FLAM and driven by climate change scenarios until the year 2100; (iv) simulation of adaptation options under the worst-case scenario. The modeling results show an increase in burned areas under all Representative Concentration Pathway (RCP) scenarios. Maintaining current temperatures (RCP 2.6) will still result in an increase in burned area (total and forest), but in the worst-case scenario (RCP 8.5), projected burned forest area will more than triple by 2100. Based on FLAM calibration, we identify hotspots for wildland fires in the boreal forest and suggest adaptation options such as increasing suppression efficiency at the hotspots. We model two scenarios of improved reaction times—stopping a fire within 4 days and within 24 h—which could reduce average burned forest areas by 48.6% and 79.2%, respectively, compared to projected burned areas without adaptation from 2021–2099.

Keywords: wildfire modeling; climate change impacts; boreal forest; adaptation options

Citation: Corning, S.; Krasovskiy A.; Kiparisov, P.; San Pedro, J.; Viana, C.M.; Kraxner, F. Anticipating Future Risks of Climate-Driven Wildfires in Boreal Forests. *Fire* **2024**, *7*, 144. https://doi.org/10.3390/fire7040144

Academic Editor: Grant Williamson

Received: 29 February 2024
Revised: 11 April 2024
Accepted: 12 April 2024
Published: 17 April 2024

1. Introduction

The boreal ecozone forms a circumpolar belt across northern Eurasia and North America. It primarily spans eight countries: Canada (27.5 percent), China, Finland, Japan, Norway, Russia (60 percent), Sweden (1.5 percent), and the United States (3.7 percent), and is the world's largest land biome consisting of forested and partially forested ecosystems [1]. Boreal forests are diverse hubs of biodiversity, and they thrive and provide for populations around the globe despite harsh conditions, such as short growing seasons and severe winters [2]. However, they face worsening conditions fueled by climate change and serve as a harbinger of threats to come for lower-latitude forests [3]. Global warming-induced changes to conditions in the boreal ecozone, namely rising temperatures, melting permafrost, and changing precipitation patterns, promote a fire-friendly environment. There is a knowledge gap as to how climate-driven conditions may alter wildfire dynamics by the end of the century, where the effects may be the largest, and where to focus adaptation and mitigation efforts [4].

As one of the most important natural disturbances of forest ecosystems, wildfires have a major impact on forest resources and ecological succession [5–8]. A general review of wildfire studies was carried out by [9], which highlighted the increasingly important role of climate change on the frequency and impact of extreme events such as wildfires in boreal forests and on their functions, and discussed potential adaptation options, such as silvicultural approaches, prescribed burning, and fire response. A forest fire-focused review by Li et al. corroborated that the increase in fire frequency and impact in the boreal region is resulting from climate change, and that innovative research is needed to continue addressing these changes [10]. Although a higher number of fires have been recorded in the tropics or temperate zone than the boreal zone per the European Space Agency's (ESA) MODIS FireCCI51 product [11,12], the issue of boreal fires is one of global concern due to their role in the global carbon cycle [13]. In light of recent catastrophic fire seasons across the boreal zone, including Canada [14], Sweden [15], and Siberia [16], there is a strong need to address this gap in the realm of wildfire research.

The growth and decomposition processes of trees in high-latitude regions are relatively slow due to cold climates and short growing seasons, resulting in large stocks of dead wood and soil carbon and potential disturbance feedback effects on CO_2 [17–19]. Typically, boreal fires account for about 10 percent of global fire-related carbon dioxide emissions. Studies highlighting the contribution of boreal wildfires to global carbon dioxide emissions include [13,20,21].

In 2021, however, boreal fires accounted for nearly 25 percent of fire-related carbon dioxide emissions. Atypical water deficits in both North America and Eurasia [22], as well as high temperatures, resulted in fire-conducive conditions and contributed to the devastating fires that year. Over the last five decades, Arctic temperatures have risen three times faster than elsewhere on earth [23], with wildfires contributing indirectly to the rise in temperatures through increased emissions [10]. There are few to no scenarios which show an improvement in boreal climatic conditions as they pertain to fire-conducive conditions. Rather, overwhelmingly, climate projections predict continued warming and changes to precipitation patterns in a manner which will promote wildfire occurrence and spread [24]. These changes are evident in the Siberian Taiga [25] and are projected to intensify in Canada under climate change [26]. Severe fire weather conditions are projected in central Russian and western Canadian boreal forests towards the end of this century [27]. It is therefore reasonable to expect boreal forests to become even more susceptible to devastating wildfires, barring human intervention.

One method with which to address this threat is through the modeling of historic boreal forest fires and projection of future risks under various climate change and management scenarios. Modeling aids in the identification of areas with a high probability of fire (hotspots); provides an ability to assess the vulnerability of boreal forests to fire, guide mitigation and management strategies, and optimize possible interventions; and is an important step for the Arctic in estimating the hydrocarbon budget [28]. Accurate modeling of boreal fires will allow policy-makers, government agencies, land managers, and other stakeholders to make informed decisions and act accordingly.

Global fire models tend to underestimate fire areas, especially the large-scale fires we have witnessed in recent years [29]. This could be attributed to the quickly changing and extreme conditions. There are a number of methods with which researchers are attempting to resolve this discrepancy, from utilization of machine learning methods to changing model structures [19]. In this study, we apply the wildfire climate impacts and adaptation model (FLAM) to the boreal zone. Using a process-based parameterization algorithm [30] coupled with Fine Fuel Moisture Code (FFMC) computation [31], FLAM utilizes both ignition probability and suppression efficiency to predict burned area. The ability to calibrate for low suppression efficiency, versus setting a set parameter value, allows FLAM to capture the full extent of wildfires in diverse conditions. FLAM has been successfully applied in Europe [32,33], South Korea [34], and Indonesia [35], among other locations.

Meteorological modeling and wildfire risk assessment, including the use of remote sensing and satellite imagery, have advanced significantly [36–38]. In order to understand and address the growing threat of large-scale wildfires in boreal forests and the boreal zone as a whole, as well as to contribute to the research on wildfires in the boreal zone, we applied FLAM in this region using the most recently available remote sensing data. One of the most reliable and widely used products is the Moderate Resolution Imaging Spectroradiometer (MODIS) [11,12,39–41], which has been playing an essential role in fire detection for more than a decade and remains an invaluable tool for scientists and decision-makers [42–45]. This paper provides an overview of recent and current boreal climate and burned area conditions; an analysis and comparison of burned area projections under four Representative Concentration Pathway (RCP) scenarios [46]; and a possible adaptation option to reduce burned area under RCP 8.5, an extreme scenario with the highest impact on climate and burned area by the end of the century [47]. We establish baseline understanding for wildfire dynamics in the boreal zone and set the stage for future research on this topic.

2. Materials and Methods

2.1. Study Area

The boreal zone can be divided into eight land cover classes: forests, forest mosaic (mosaic of forests and herbaceous vegetation), shrublands, grasslands, mosaic (mosaic of forests, grass-, and shrublands), croplands, lichens and moss, and sparse vegetation [11]. These are filled with diverse ecosystems, ranging from barren, arctic heathlands areas under year-round snow or ice cover and dense, forest covered peatlands, to dry grasslands and shrublands [48]. The boreal zone crosses eight countries (Figure 1), meaning the management and use of forests within this ecozone are highly varied [1]. The spatial and temporal patterns of ignitions also differ, which affects the rate of spread and the potential for fire suppression [49]. In Alaska, for example, lightning is the cause of the majority of fires [50], while in Siberia, most fires are the result of human actions [51].

Figure 1. A map of the boreal zone as defined by the International Boreal Forest Association. Source: [52]. Authors' representation.

Boreal forests are defined as high-latitude forests which experience freezing temperatures for six to eight months per year, and reach heights and canopy cover of five meters and ten percent, respectively. They represent 30 percent of global forests, of which nearly one-third is underlain by permafrost. They are composed primarily of coniferous species (pine, spruce, and fir) and secondarily of broadleaf species (namely, poplar and birch) [2], which is a result of short growing seasons and low mean temperatures [1]. Boreal forests offer critical services at all spatial scales, from food and medicine for indigenous and local communities, to paper, lumber, and a massive carbon store for global populations.

2.2. Climate Change Scenarios

The main drivers of wildfires include vegetation, climate, and human activity [53]. Hot, dry conditions promote a fire-prone environment in both fire-resilient and fire-susceptible ecosystems (or, ecosystems adapted to regular fire events and ecosystems which do not normally experience fire events, respectively) [24,53,54]. Changes in average annual temperature and annual precipitation are therefore of great interest when considering wildfire probability and burned areas in the future.

The focus of this study was to analyze the impact of these changes in climatic conditions on wildfires. Specifically, we looked at how projected temperature and precipitation influence projected wildfire occurrence and burned area. To achieve this, we conducted our study as a type of "what if" baseline scenario; what if all conditions remained the same, and the only variables to change were climatic (temperature and precipitation)? We assumed all non-climatic variable values mirrored those of recent or current conditions, with the exception of temperature and precipitation. While lightning is an important weather variable to consider in regards to wildfire ignition, especially under climate change, the scope of this study did not encompass the complexities associated with accurate long-term lightning trend modeling [55], especially considering the focus on multiple climate change and adaptation scenarios utilized.

Due to our focus on weather and climate, we did not couple our fire model with any vegetation or population model and therefore are not able to appropriately assess the interplay between variables (e.g., loss of fuel due to prior fire occurrence).

We investigated the impacts of climate change on modeled burned areas in the boreal zone under four Representative Concentration Pathway (RCP) scenarios: RCP 2.6, RCP 4.5, RCP 6.0, and RCP 8.5 [46]. RCP 8.5 is considered a "baseline" scenario, without any specific climate mitigation target. Greenhouse gas emissions and concentrations in this scenario increase significantly over time, resulting in radiative forcing of 8.5 W/m^2 at the end of the century. The RCP 4.5 and RCP 6.0 scenarios represent a stabilization approach, where the radiative forcing level stabilizes at 4.5 W/m^2 and 6 W/m^2, respectively, before 2100 through the implementation of a range of technologies and strategies to reduce greenhouse gas emissions. The RCP 2.6 emission and concentration pathway aligns with the literature on mitigation scenarios aiming to limit the increase in global mean temperature to 2 °C.

For modeling, climate data were taken from the Inter-Sectoral Impact Model Intercomparison Project (ISIMIP2b) [56], which provides daily global climate variables globally at 0.5 degree resolution and covers the following time periods: pre-industrial (1661–1860), historical (1861–2005), and future (2005–2100). Future conditions are based on results from the Coupled Model Intercomparison Project 5 (CMIP5), upon which the ISIMIP2b data are based.

To better understand how climate has influenced wildfire probability and burned area in future scenarios, we used annual mean temperature and annual precipitation from the Hadley Centre Global Environment Model version 2 (HadGEM2-AO) [57]. HadGEM2 is a coupled Earth System Model used by the Met Office Hadley Centre for CMIP5 centennial simulations as part of the high-resolution CHELSA dataset [58]. These data were used to visualize the average predicted temperature and precipitation values during the historical (1979–2013) period (Figures 2 and 3, respectively). The annual mean temperature [°C] and annual precipitation [mm per year] were used to calculate the difference (deltas) in

projected annual mean temperature and precipitation between the historical period and two future periods (2041–60 and 2061–80), which provide valuable information on future hotspots in terms of higher temperatures and lower precipitation across the study area (Figures to be added). This study was more focused on mid-late century changes in climate, which is why the period 2021–2040 was not visualized.

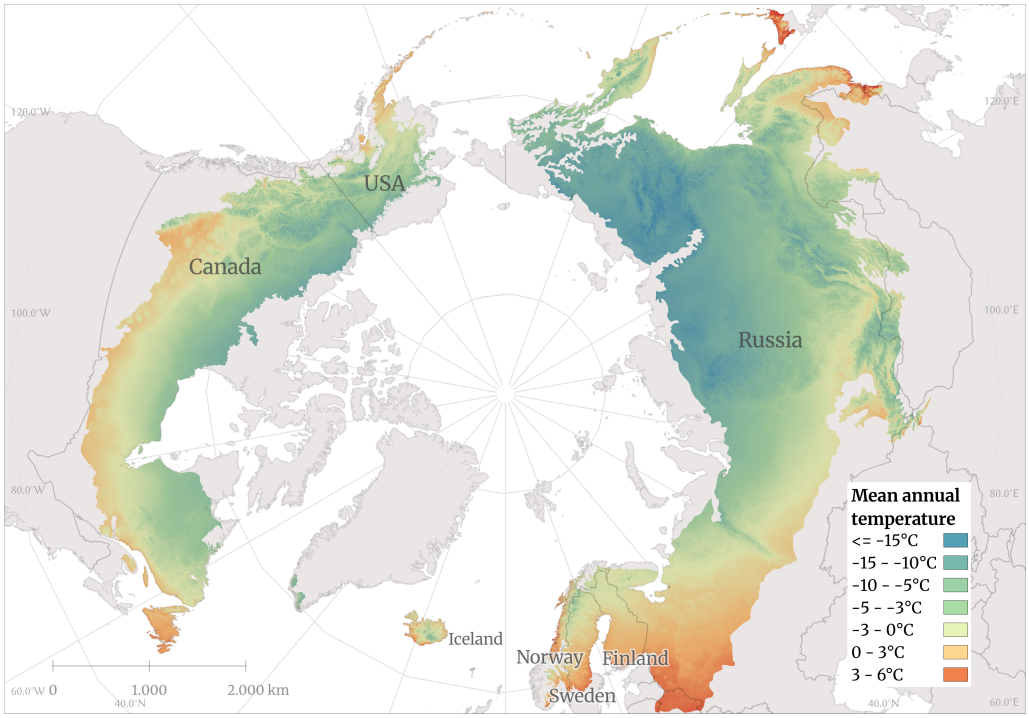

Figure 2. Historical (1979–2013) mean annual temperature in degrees Celsius for the boreal zone, native 1 km^2 resolution. Source: [58]. Authors' representation.

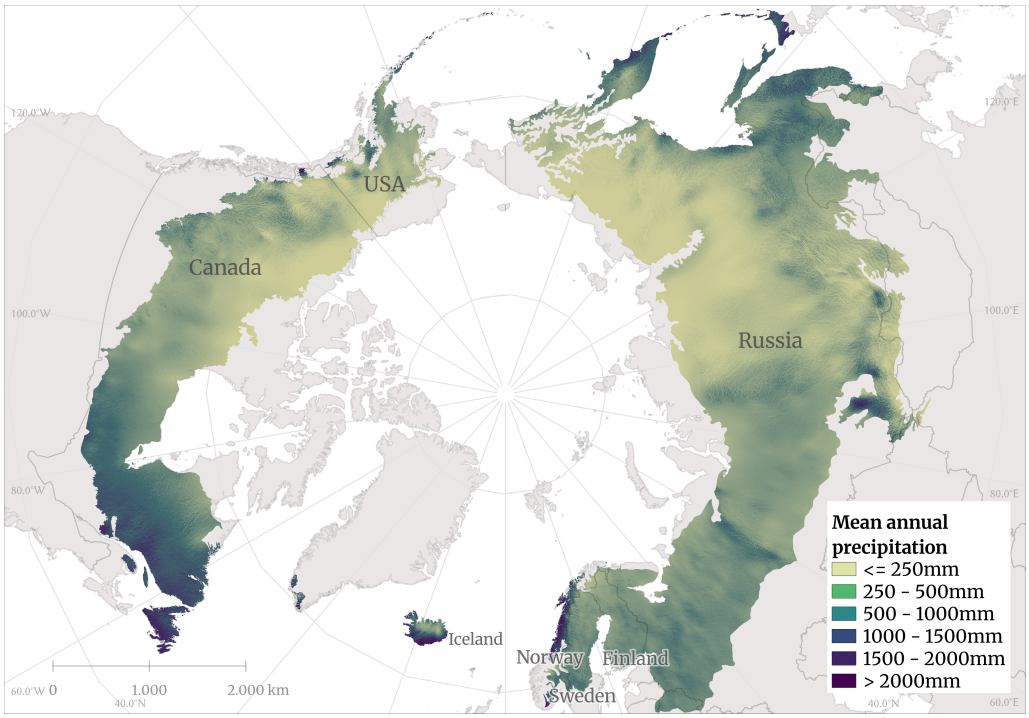

Figure 3. Historical (1979–2013) mean annual precipitation in mm for the boreal zone, native 1 km^2 resolution. Source: [58]. Authors' representation.

2.3. FLAM Model

The Wildfire Climate Impacts and Adaptation Model (FLAM) employs a mechanistic framework that integrates a process-based fire parameterization algorithm, capturing the influences of climate, fuel, topography, and human activities on wildfire probability, frequency, and burned area. It operates on a daily time-step and uses relative datasets to define past and future wildfire trends. FLAM flowchart is given in Figure 4. It is highly adjustable and adaptable, which allows for the inclusion of additional fire-related input variables to enhance its precision in portraying local and regional fire dynamics under different scenarios [32,34,35]. The climate impacts in FLAM are modeled based on daily weather conditions. Fine fuel moisture content is assessed using the Fine Fuel Moisture Code (FFMC) computation [31], coupled with the Arora and Boer algorithm [30].

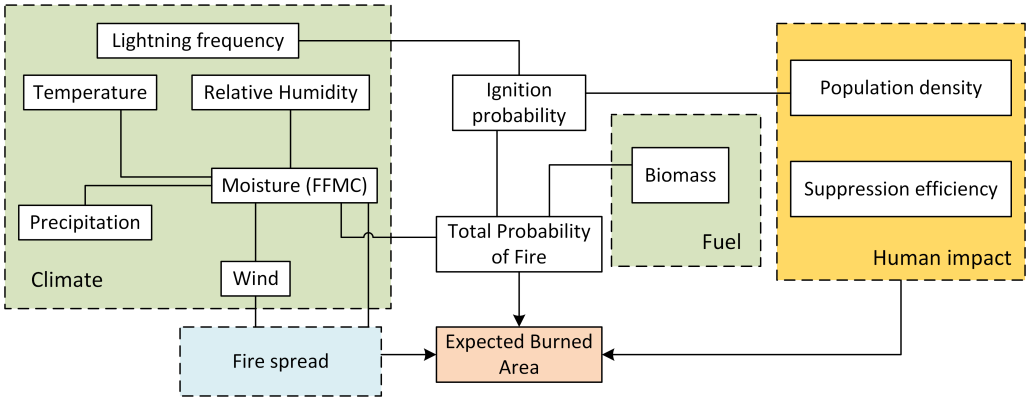

Figure 4. The FLAM workflow.

2.4. FLAM Input Data

FLAM was originally run at 0.5 degree resolution [35] to produce burned area projections for the period 2001–2100, considering four different RCP scenarios: 2.6, 4.5, 6, and 8.5. Therefore, all other input data were resampled to this resolution during pre-processing. Additionally, two adaptation scenarios were devised to investigate the effects of enhancing fire suppression efficiency on burned area in RCP 8.5. To perform the necessary analysis and calibration processes, FLAM utilizes data for several key variables, found in Table 1. All non-climatic variables (plus lightning) were kept static for future predictions to focus on the impacts of climate change on burned area and fire dynamics.

Table 1. Input data required by FLAM.

Variable	Unit	Frequency	Source
Temperature	Degrees Kelvin/°C	Daily	Meteo climate data
Wind speed	m/s	Daily	Meteo climate data
Precipitation	Meters	Daily	Meteo climate data
Lightning	Flashes/km^2/month	Monthly	HRMC
Relative humidity	%	Daily	Meteo climate data
Fuel	gC/m^2	Once or yearly	G4M/ Copernicus
Landcover	Type	Once or yearly	ESA World Cover
Population density	People/km^2	Once or yearly	GPW v4
Observed burned area	ha	Monthly	MODIS FireCCI51

2.4.1. Population and Lightning Data

Population density data are used to calculate the human ignition probability and an initial fire suppression efficiency value. Population density data were acquired from the Gridded Population of the World dataset v4 [59]. Population grids at 5-year intervals for the period 2000–2020 were used, and 2020 values were kept constant for future projections.

For lightning frequency, the monthly climatology from 1995–2014 at 0.5 degree resolution from LIS/OTD Gridded Lightning Climatology Data Collection Version 2.3.2015 [60] was averaged to produce a static lightning strike map used for historical and future projections. This represents the natural ignition source of wildfires in the model.

2.4.2. Burned Area, Biomass, and Landcover Data

Observed burned areas were extracted from the FireCCI51 burned area product v5.0, created within the European Space Agency's Climate Change Initiative (CCI) Programme, for the period 2001–2020 [11,41]. Observed burned area data were used for analysis of modeled past and present burned area, as well as for calibration of FLAM and comparison of the historical period to future projections.

Fuel in the form of biomass is necessary to calculate fire ignition and spread. Biomass, used to represent fuel available to burn, was obtained from two sources. For forested areas, biomass values were taken from the G4M model at a resolution of 0.5 degrees [61]. G4M computes forest biomass based on land cover and biomass maps, and is used as a basis for the precision and reliability of the model outcome. For all non-forested land cover types, biomass was obtained from Copernicus Above Ground Biomass Global product [12]. A simple proportional equation was used to calculate the pools of coarse woody debris and litter from the biomass values. Biomass was static for this study; therefore, the values used in FLAM were uniform across the study period (2001–2099).

Land cover data play a crucial role in the assessment of wildfire behavior in different land cover types, which helps in further understanding wildfire dynamics in the boreal zone. Land cover data were acquired from the European Space Agency (ESA) CCI MODIS land cover map for 2010 [41], which was used for both historical modeling and future projections. The map contains 19 1st-level land cover categories which we recategorized into forest and non-forest classes. Land cover numbers 50–90 were clustered as forest, and the remaining classes were grouped into the non-forest category (excluding lichens and mosses, and water). The forest land cover was further sub-categorized by forest type: broadleaf, needleleaf (deciduous), needleleaf (evergreen), and mixed leaf.

2.4.3. Model Calibration and Validation

One key feature of FLAM is the ability to calibrate the spatial fire suppression efficiency to better capture inter-annual burned area dynamics of historical burned area. FLAM is calibrated by comparing actual and modeled burned areas aggregated over time. Throughout the calibration period, FLAM parameters are adjusted to match the average burned area per pixel. Pixels impossible to calibrate are systematically removed to mitigate errors in projections. These pixels are typically those with insufficient fuel available to burn or lacking an ignition source.

Post-calibration, the model undergoes re-evaluation with a focus on annual comparisons of burned areas. This simplified calibration approach guarantees the alignment of burned areas in the historical period across all RCPs. The validation phase of FLAM involves testing its accuracy in modeling yearly burned area.

2.4.4. Burned Area Projection and Adaptation Scenarios

Using the calibrated model results, we generated future burned area predictions under various climate change scenarios. Given that lightning and all of the non-climatic variables were assumed constant for the projection period, the projected burned areas can be interpreted as a "what if" situation in regards to climate change, hypothesizing the state of wildfires if present-day conditions were maintained but weather conditions reflected conditions as projected under various climate change scenarios. This provides insight into how wildfire occurrences and regimes would play out in a changing climate (the RCP scenarios), assuming continuity in current management strategies and lightning frequency.

Using the burned area projections from FLAM, we can identify fire hotspots: areas which have a high likelihood of burning, severe fires, and/or a low suppression efficiency.

In addition to the four RCP scenarios, in this paper, we wanted to show that changes to conditions other than climate and weather could impact modeled burned areas. Therefore, we established a fifth and sixth scenario to explore two adaptation options.

FLAM is calibrated using spatial suppression efficiency based on the observed average burned areas [35]. For our adaptation scenarios, we chose to represent an intervention through the modification of suppression efficiency. Suppression efficiency of a fire can be improved in a number of ways: quicker detection of and reaction to a fire, more available resources, and targeted forest management to improve intervention effectiveness, to name a few. We wanted to show how increasing suppression efficiency in FLAM-identified hotspot areas could reduce the total burned area. To highlight the impact of such an intervention, we compared results under RCP 8.5.

We considered two "what if" options in which we assumed that the suppression efficiency in hotspots (where $q < q_a$, $q_a \in (0, 1]$ is a threshold, with q representing suppression efficiency) could be improved such that all fires were suppressed within a certain number of days after ignition. Mathematically, this can be expressed in the following way. Let Q be the matrix of suppression efficiency values $q_{ij} \in (0, 1], i = 1, \ldots, M,\ j = 1, \ldots, N$, where M is a number of rows and N is a number of columns. This matrix represents a geospatial grid covering the study region, where indices (i, j) are the coordinates of a grid cell, and therefore, q_{ij} represents the q value of the cell found at (i, j). As an adaptation option, we make the following transformation of the elements of matrix Q:

$$q_{ij} := \begin{cases} q_a, & \text{if } q_{ij} < q_a, \\ q_{ij}, & \text{elsewhere.} \end{cases} \tag{1}$$

Here, q_a is constant threshold, i.e., it is the same for all grid cells. Recall that the expected fire duration for each grid cell (i, j) is calculated according to the following equation [35]:

$$\bar{\tau}_{ij} = \frac{1 - q_{ij}}{q_{ij}}. \tag{2}$$

We consider two adaptation scenarios, increasing suppression efficiency at the hotspots according to Equation (1) with $q_a = 0.5$ corresponding to suppressing a fire in one day, and $q_a = 0.2$ corresponding to expected fire duration of 4 days (Equation (2)).

3. Results

3.1. Wildfires in the Boreal Zone: Past and Present

From 2001 to 2020, over 251 Mha of the boreal zone burned, or approximately 12.6 Mha per year. Figure 5 shows the breakdown of the burned area per year and per vegetation class. The vast majority (≈88%) of the burned area was classified as forests (≈65%), grassland (≈13%), or a mosaic of forests and herbaceous vegetation (≈10%). Four other land cover classes (cropland, shrubland, lichens and moss, and a mosaic of forests, grass-, and shrublands) made up the remaining 12% of burned area. The forest land cover class can be further broken down into needleleaf (evergreen), needleleaf (deciduous), broadleaf, and mixed leaf. Of the burned forested area, 82% was of the type needleleaf (58% and 24% for deciduous and evergreen, respectively), 16% was broadleaf, and only 2% occurred in mixed leaf forests.

Separating this period into two decade-long segments (2001–10 and 2011–20) highlights the impact of an abnormally large fire which occurred in Russia in 2003, during which 27.3 Mha of primarily forested area burned—more than double the yearly average burned area for the 20-year period. Table 2 shows the burned area per decade, per vegetation class, and the percentage of the total burned area for which that vegetation class accounted. In the first decade, 61% of burned area was classed as forest, 14.5% as grassland, and 10.5% as mosaic (forest/herbaceous). In the second decade, 68% of burned area was forest, 11.5% as grassland, and 9.4% as mosaic (forest/herbaceous). Most notably, there is a 7% increase in the proportion of burned area which is classed as forest. A similarly important trend is seen

when comparing the types of forests burning between the two decades. From 2001 to 10, broadleaf forests comprised 20% of burned forest area and needleleaf 77% (56% deciduous, 22% evergreen). In comparison, from 2011 to 20, broadleaf forests comprised only 12% of burned forest area, with both types of needleleaf forests experiencing a 4% increase in their share of burned area.

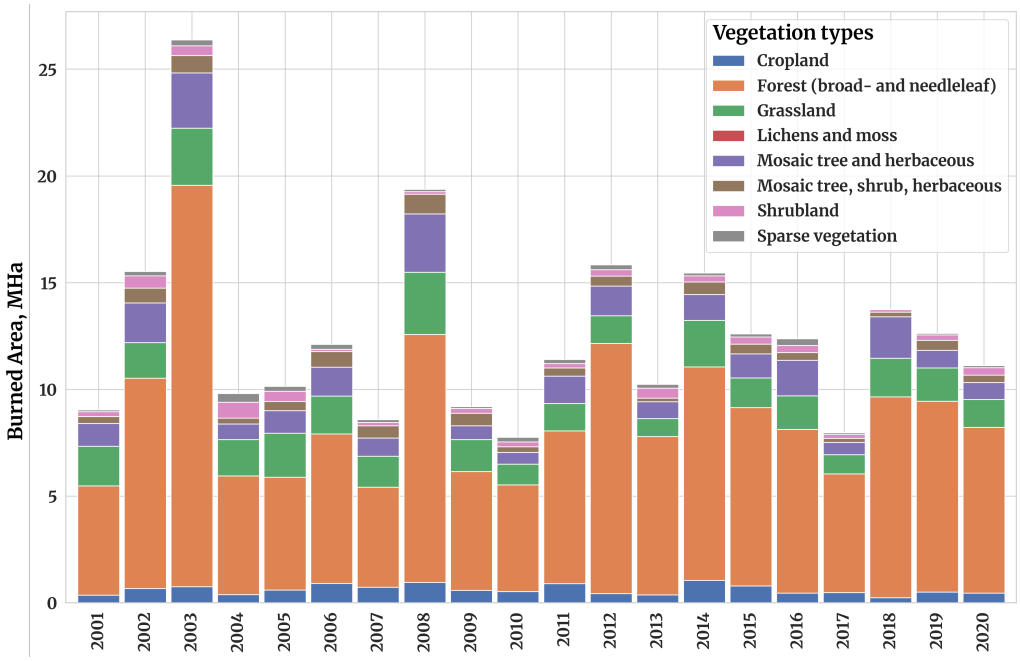

Figure 5. Burned area vegetation dynamics in the boreal zone (2001–2020). Source: [41]. Authors' representation.

Table 2. Total burned area per vegetation class per 10-year period (in descending order by MHa; italicized volumes and percentages in brackets are part of the forest class) based on FireCCI51 dataset [41].

Classes	2001–2010 (MHa)	Percentage (%)	2011–2020 (MHa)	Percentage (%)
Forest:	78.47	61.3	84	68.0
Needleleaf—deciduous	*(43.86)*	*(55.9)*	*(50.65)*	*(60.3)*
Needleleaf—evergreen	*(17.6)*	*(22.4)*	*(21.96)*	*(26.1)*
Broadleaf	*(15.74)*	*(20.1)*	*(10.11)*	*(12.0)*
Mixed leaf	*(1.27)*	*(1.6)*	*(1.27)*	*(1.5)*
Grassland	18.56	14.5	14.15	11.5
Mosaic tree, herb	13.41	10.5	11.6	9.4
Cropland	6.51	5.1	5.68	4.6
Mosaic tree, shrub, herb	5.67	4.4	3.66	3.0
Shrubland	3.31	2.6	2.83	2.3
Sparse vegetation	1.96	1.5	1.45	1.2
Lichens and moss	0.13	0.1	0.14	0.1
Total	*128.02*	*100*	*123.51*	*100*

When looking specifically at burned forest area in the boreal zone (i.e., boreal forests) in Figure 6, there are slight differences visible in the spatial spread of burned pixels. In the first decade, the large Russian fire of 2003 dominates the burned pixels in southern Russia. There are some burned forests in central and northern Russia, central Canada, and southern Europe, but the pixels designating burned forests are largely absent from the far north of the boreal zone. In the second decade, there is a general trend for more central, borderline northern boreal forests to burn. This is more clearly seen in Figure 7, which shows the difference in burned area between the later, more recent decade (2011–20) and the earlier decade (2001–10), with red highlighting where more boreal forests have burned recently as

opposed to at the beginning of the century. Fires are moving north within the boreal zone. Both figures show burned area in the original resolution of 0.25 degrees, though it should be noted that in modeling, the data were aggregated to a resolution of 0.5 degrees.

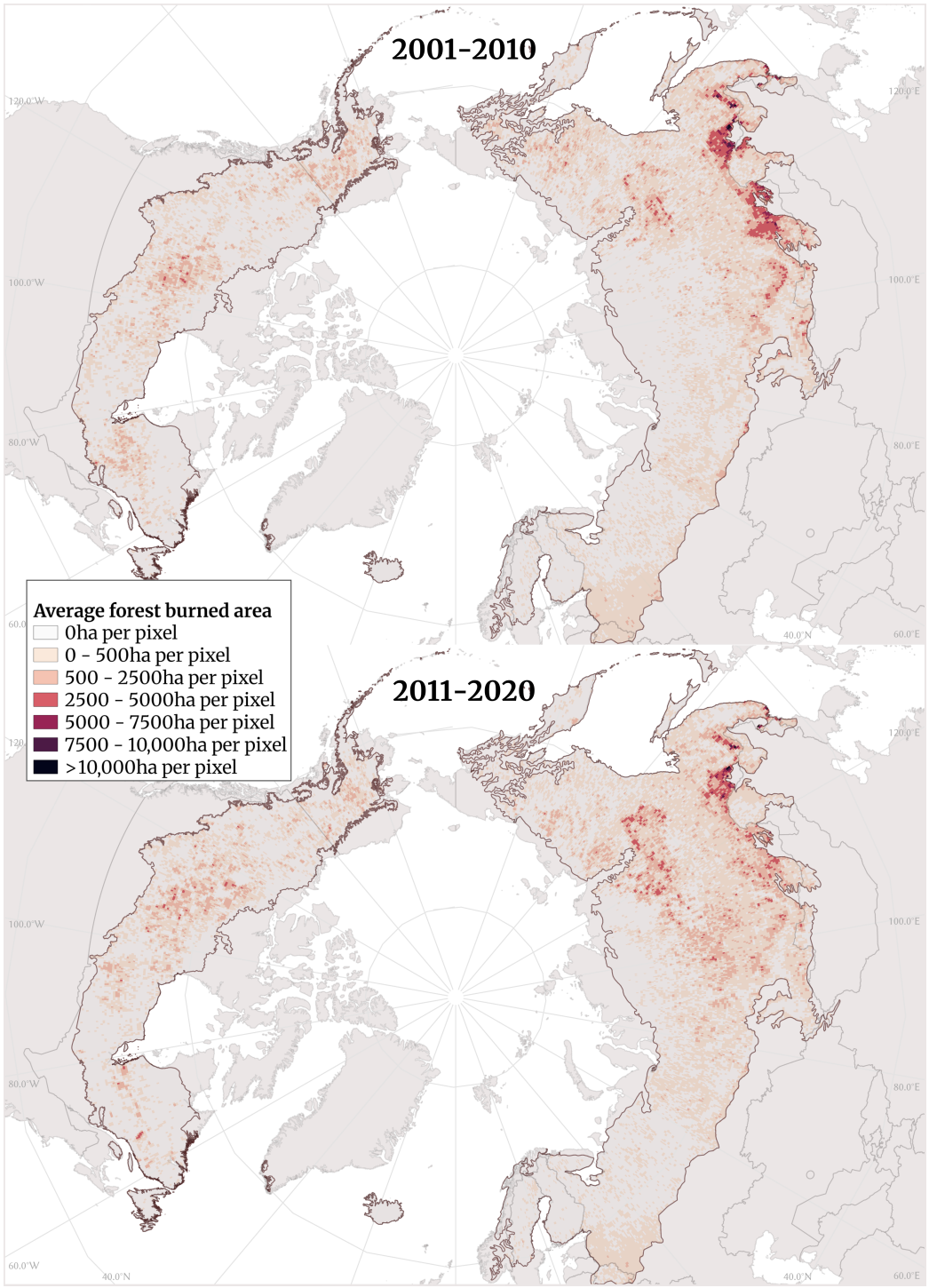

Figure 6. Burned area in boreal forests over two decades (2001–2010 and 2011–2020), native 0.25 degree resolution. Source: [41]. Authors' representation.

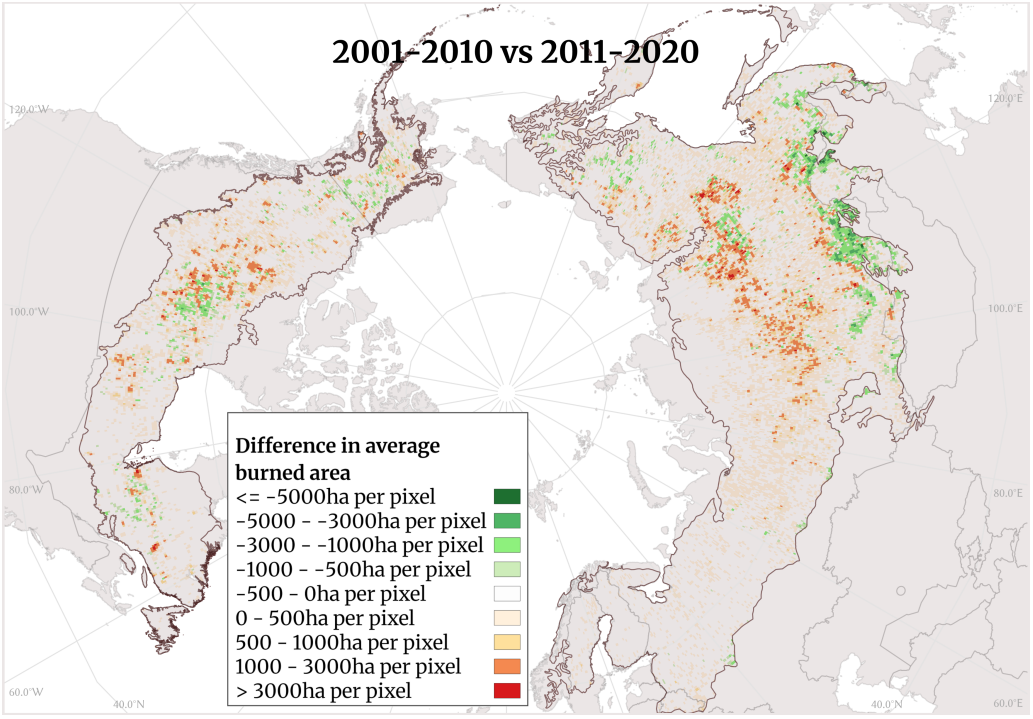

Figure 7. The difference in burned area in boreal forests between two decades (2011–2020 compared to 2001–2010), native 0.25 degree resolution. Source: [41]. Authors' representation.

3.2. FLAM Calibration and Sensitivity Analysis in the Context of RCP Scenarios

For calibration, we chose the 10-year period spanning from 2011 to 2020. FLAM was forced to reproduce the average burned area over the entire period, as opposed to each individual year. During the calibration process, FLAM did not utilize any information regarding interannual variability but relied solely on the yearly average burned areas and their locations over a 10-year period. To validate the calibration, we then compared the FLAM-modeled burned areas with those from the FireCCI51 data [41]. The calibrated outputs from FLAM exhibit variability in different years across the RCP scenarios, although all FLAM RCP projections fit the 10-year average burned area. Overall, FLAM output generally mirrored the trends in observed burned area obtained from FireCCI51, and the lower and upper bands of the predictions did a good job of capturing the observed burned areas from FireCCI51, implying that the model is able to reflect observed conditions despite variability under various climate change scenarios.

Figure 8a illustrates the yearly modeled burned area sums across all RCPs from 2011 to 2020. FLAM output varies with respect to each RCP scenario due to differences in daily weather-related variables, although the average across the entire period is the same across scenarios. While a single FLAM RCP scenario does not perfectly correlate with observed yearly sums, it is always possible to select a scenario which is closest to the actual burned area sum for each given year.

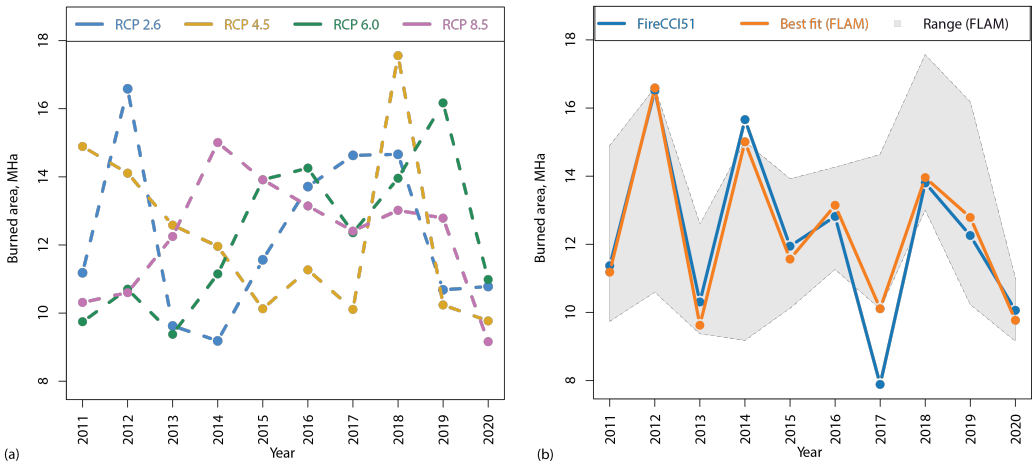

Figure 8. (**a**) Calibrated FLAM results across RCPs. (**b**) "Best fit" of FLAM predictions compared to FireCCI51 data, with upper and lower bounds (range) of FLAM predictions.

The ability of FLAM to model burned area is best seen in Figure 8b, which shows the yearly FireCCI51 burned area sum (blue), the upper and lower bounds of FLAM predictions across the four scenarios (shaded area), and a "best fit" (BF) approximate (orange), calculated as follows:

$$N^*(year) = \underset{N \in \{2.6, 4.5, 6.0, 8.5\}}{\operatorname{argmin}} \left| \mathrm{FireCCI51}(year) - \mathrm{FLAM}_N(year) \right|,$$

$$\mathrm{BF}(year) = \mathrm{FLAM}_{N^*(year)}(year), \quad \text{where} \quad year \in [2011, 2012, \ldots, 2020].$$

Here, BF is the values of burned area for the "best fit" line, N is the number of RCP scenario, $\mathrm{FLAM}_N(year)$ is burned area modeled by FLAM in a given year under RCP scenario N, $\mathrm{FireCCI51}(year)$ is the burned area reported by MODIS for a given year, and $N^*(year)$ is the best-fitting RCP for a given year. In other words, we consider all FLAM RCP burned area sums each year and select the value which most closely resembles the FireCCI51 value. These are then connected by a line to create a "best fit" line.

Runs under RCP 2.6 best captured the years 2011–2013 and 2015, RCP 4.5 showed the closest fit for years 2017 and 2020, RPC 6.0 captured year 2018, while RCP 8.5 captured years 2014, 2016, and 2019. Over the span of 10 years, RCP 2.6 exhibited the best fit for 4 years, RCP 4.5 for 2 years, RCP 6.0 for 1 year, RCP 8.5 for 3 years. This illustrates the uncertainty in climate forcing estimates as provided by the RCPs and highlights the model's capacity to reflect complex climatic interactions. Overall, the correlation between the best fit (orange line) and observations (blue line) is assessed with Pearson's r equal to 0.95. Figure 8b shows that overall, FLAM was able to capture large fires; the only obstacle was capturing the relatively small area (on average) burned in 2017.

A comparison between FLAM output driven by individual climate scenarios and FireCCI51 burned area reveals a clear disparity in values. Table 3 presents Pearson's correlation coefficients and Mean Absolute Errors (MAE) in MHa for the four FLAM RCP scenarios as compared to the FireCCI51 dataset. As previously mentioned, the "best fit" line exhibited the highest correlation with the FireCCI51 dataset and the lowest MAE compared to the individual scenarios, with a Pearson's r value of 0.95 and MAE of 0.55 MHa. Among the individual scenarios, RCP 4.5 exhibited the highest Pearson's correlation with FireCCI51, with $r = 0.45$, albeit accompanied by a high MAE value of 2.35 MHa. Both RCP 2.6 and RCP 8.5 demonstrated better MAE performance, each of which had an MAE equal to 1.86 MHa, though their Pearson's coefficients were relatively low, at $r = 0.2$ and $r = 0.27$, respectively. In contrast, RCP 6.0 displayed the poorest performance with Pearson's $r = 0.06$ and MAE of 2.57 MHa. The clear disparity in values between individual

scenarios emphasizes the challenges associated with accurately capturing the variable influence of different drivers and their interactions in fire modeling.

Table 3. Pearson's correlation coefficient and Mean Absolute Error (MAE) in MHa for the 4 FLAM RCP scenarios and "best fit" as compared to the FireCCI51 dataset [41].

Scenario	Pearson's *r*	MAE, MHa
RCP 2.6	0.20	1.86
RCP 4.5	0.45	2.35
RCP 6.0	0.06	2.57
RCP 8.5	0.27	1.86
Best fit	0.95	0.55

It is worth noting that 4% of the area identified by FireCCI51 as burned area in pixels could not be calibrated by FLAM. The inability to calibrate is often due to one of two data conditions. First, in areas classified as urban/developed, especially in or near cities, the lack of fuel available for burning is a common issue due to coarse-resolution data. When land cover is categorized as urban/developed, the model assumes that there is no fuel available for burning. Addressing this limitation was beyond the scope of this study, as there are no studies that equate urban and developed land to a comparable above-ground biomass value. Second, the lack of an ignition source, whether natural (such as a lightning strike) or anthropogenic (probabilistically determined by population density vs. suppression efficiency), may hinder FLAM's ability to predict fire or burned area. To mitigate errors in projections due to unavailability of data in these areas, the corresponding pixels are systematically removed.

3.3. Future Climates

To better understand the changing climate in the boreal ecozone, we visualized mean annual temperature [°C] and accumulated precipitation [mm/year] for a historical period (1979–2013) and two future periods (2041–60 and 2061–80) under four RCP scenarios (RCP 2.6, 4.5, 6, and 8.5) with the CHELSA GCM HadGEM2-AO dataset. Historical temperature and precipitation were processed and visualized to establish baseline values (Figures 9 and 10).

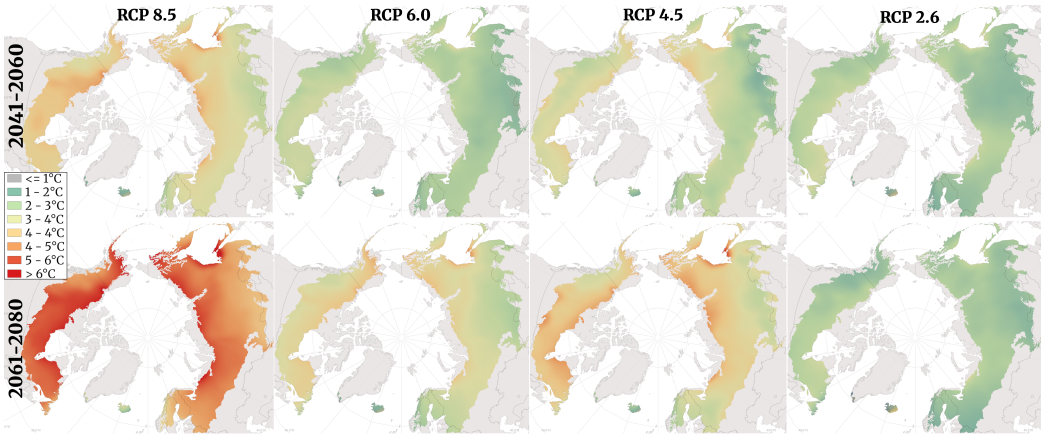

Figure 9. Change in mean annual temperature in degrees Celsius for the boreal zone as compared to the historical period (1979–2013), native 1 km^2 resolution. Source: [58]. Authors' representation.

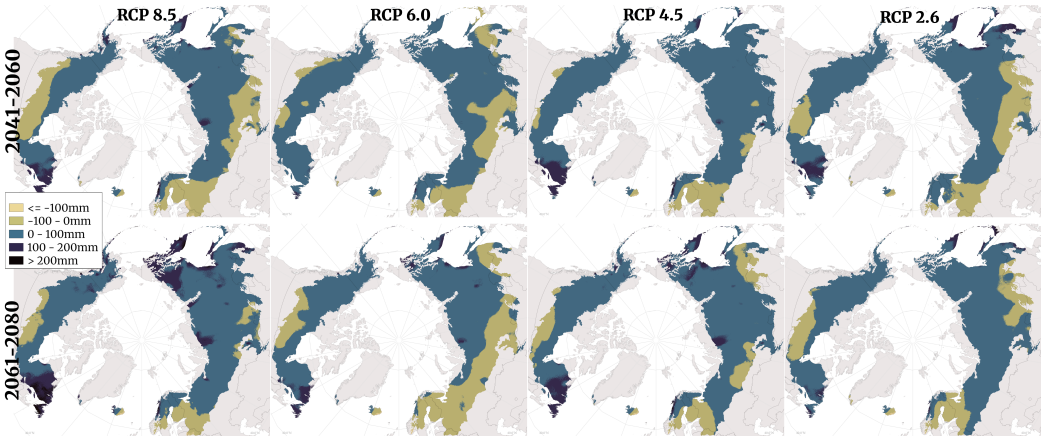

Figure 10. Change in mean annual precipitation in mm for the boreal zone as compared to the historical period (1979–2013), native 1 km^2 resolution. Source: [58]. Authors' representation.

For each future period and RCP scenario, climate data were (1) processed to analyze future (projected) conditions, then (2) compared to the baseline results from the historical period for the entire boreal ecozone to (3) calculate the delta (change) in value between the historical and future time periods.

3.3.1. Temperature

The boreal zone is expected to experience rising temperatures by the end of the century under all scenarios, but there are significant differences between scenarios. Warming is projected to be greater in the high-latitude regions of the boreal zone under all RCPs, particularly in the North American continent and over large areas of Russia. In more mid-latitudes, especially in Europe, a smaller amount of warming is predicted. These trends are visible in RCP 2.6, RCP 4.5, and RCP 6.0, and are strongly evident in RCP 8.5. Already in the period 2041–60, the differences between the scenarios become apparent. Under RCP 2.6, most of the boreal zone will warm by 1–2 degrees, with notable exceptions in the northern boreal zone of Canada, western Siberia, and the area around the Sea of Okhotsk in the Far East of Russia (which will warm by more than 3 degrees) and western Europe (with temperature changes between 0 and 1 degree). Iceland will experience an increase of 0 to 1 degree in the west of the island and up to 3 degrees in the east. Under RCP 4.5, some regions are expected to warm by up to 5 degrees, with much of the boreal zone in North America and the Far East expected to warm by at least 3 degrees. Under RCP 6.0, the spatial pattern of warming is similar, but more moderate. Rising temperatures are even more prevalent under RCP 8.5, which predicts 4–5 degrees of warming at the highest latitudes, especially in the Northwest Territories of Canada and the entire northern area of the Russian boreal zone, as well as along the coast of the Sea of Okhotsk, with only sparse areas at the southern extreme of the boreal zone warming by less than 4 degrees.

By 2061–80, the differences between the scenarios are even more pronounced. Under RCP 2.6, there are minimal differences between 2041–60 and 2061–80, with slightly more warming in Siberia, implying a relatively stable climate in the boreal ecozone by mid-century. Under RCP 4.5, over half of the total boreal zone and almost all of the boreal zone in North America appear to experience at least 4–5 degrees of warming. However, the more mid-latitudes of Asia and southwest of the Yukon in Canada and part of Alaska see a more moderate increase of 3 degrees. The RCP 6.0 scenario for 2061–2080 also shows a more moderate temperature increase compared to RCP 4.5. Under RCP 8.5, the entire boreal zone, except Iceland and parts of Norway and Sweden, will warm by 5 degrees or more.

3.3.2. Precipitation

Projected changes are more variable and less certain for precipitation in the boreal zone under all four RCPs. In general, the largest changes in precipitation are expected under RCP

8.5 and the least extreme changes are expected under RCP 2.6. There is a trend over time and across scenarios towards drier conditions in the southern-most areas of the boreal zone, mainly in Russia, Canada, and the Scandinavian countries (most pronounced in Finland). The differences in projected precipitation become larger over time between the scenarios. In other words, the difference in expected precipitation, for example, is greater between RCP 2.6 and 4.5 than for either scenario in 2041–60 compared to 2061–80 values. Similarly, in northern Canada, annual precipitation is expected to increase across all scenarios, with the largest increases expected under RCP 8.5 in the northwest of the country.

Precipitation is projected to increase over the entire territory of Russia, with the largest increases occurring in the North Siberian and Far Eastern parts of the boreal zone. Overall, more areas within the boreal zone are projected to experience an increase in precipitation than a decrease. Notable exceptions include parts of Finland, southern Russia, and southern Canada. It is noteworthy that under RCP 6.0, despite a smaller increase in temperature, there is a significant decrease in precipitation compared to all other scenarios. Precipitation under RCP 6.0 will decrease in almost the entire European part of the boreal zone, and the decrease will extend to the south of the boreal zone in both Eurasia and North America.

3.4. Burned Area Projections by FLAM

Burned area projections from 2011 to 2099 were produced by FLAM for four RCP scenarios. The results can be seen in Figure 11. The dotted line separates the calibration period (2011–2020) from the projections (2021–2099), although the entire period is modeled. Visually, the four scenarios appear similar for the first few decades, but differences in annual burned area become strongly apparent by the end of the century. In RCP 2.6, the burned area appears to remain relatively consistent over time, with a slight increase in burned area (forest and non-forest) over the next 70+ years. In contrast, we see a noticeable uptick in burned area in the three other RCP scenarios, with overall increases being the largest in RCP 8.5, followed by 6 and 4.5. Notably, non-forest burned area appears to increase more in contrast to forests in RCP 4.5, although the reason for this is unclear. In RCP 8.5, the increase in burned area starts gradually but eventually rises at an increasing rate, with a clear upward trend beyond the end of the century.

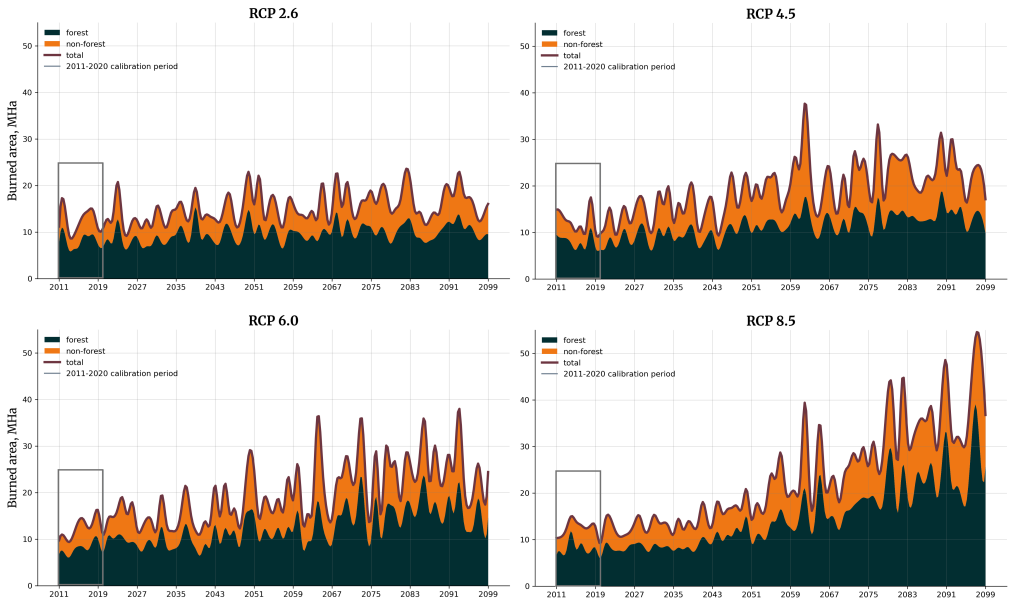

Figure 11. Burned areas in the boreal forest modeled by FLAM under four RCP scenarios. Calibration period: 2011–2020; projection period: 2021–2099.

To better assess and understand the projected burned forest area values, we calculated average annual burned forest area. The average annual burned forest area was calculated

for the 10-year calibration period to provide a baseline value with which to compare the future periods and scenario results. For projections across scenarios, the average annual burned forest area was calculated over 20-year periods.

Table 4 shows these values starting with the period 2040–2059, where there begins to be a clear visual difference between scenarios, as seen in Figure 9. As expected, the annual burned forest area increases over time and across RCP scenarios, from the best-case (RCP 2.6) to the worst-case (RCP 8.5). The difference between the average annual burned area and the historical baseline is found beneath the absolute value.

Table 4. Average annual burned forest area modeled by FLAM for each scenario in 3 future projection periods, and as compared to historical average annual burned forest area (all values in millions of hectares, MHa).

Time Period	RCP Scenario	2.6	4.5	6.0	8.5
Historical (2011–2020)	Average Annual BA	7.93 ± 1.50	7.93 ± 1.59	7.93 ± 1.32	7.93 ± 1.63
2040–2059	Average Annual BA	9.65 ± 1.92	10.44 ± 1.62	11.23 ± 3.25	11.61 ± 1.99
	Δ Average Annual BA	1.72	2.5	3.3	3.68
2060–2079	Average Annual BA	10.08 ± 1.64	12.69 ± 2.05	14.08 ± 3.06	17.25 ± 2.56
	Δ Average Annual BA	2.15	4.76	6.14	9.31
2080–2099	Average Annual BA	10.35 ± 1.72	13.59 ± 1.85	16.25 ± 3.39	24.08 ± 1.91
	Δ Average Annual BA	2.42	5.66	8.31	16.15

In the first period, the changes seen under RCP 2.6 are relatively small. In comparison, the changes observed under RCPs 6.0 and 8.5 are twice as large as those observed under RCP 2.6. In the second period (2061–2079), the differences are larger; burned area increases by about 2 Mha per scenario, with projected conditions under RCP 8.5 more than three times the change in area burned under RCP 2.6. By the third period (2081–2099), burned area appears to be more or less stabilized under RCP 2.6, with minimal increases between the second and third periods, which is also true under RCP 4.5. However, steady increases are still observed under RCP 6.0, where the average annual area burned is expected to double compared to baseline. Alarmingly, under RCP 8.5, the average annual area of forest burned is projected to triple over this period. Overall, it appears that we can expect an increase in the area burned in the boreal forest regardless of the RCP scenario, with the most devastating increases occurring under RCP 8.5.

3.5. FLAM: Adaptation Options to Combat Forest Fires in the Boreal Zone

By definition, suppression efficiency is the probability of extinguishing a fire within one day, i.e., a value of 0.5 corresponds to a fire duration of one day or 24 h. Lower values correspond to longer fire duration, up to several weeks [35]. Hotspots of lower suppression efficiency are found in Russian Siberia and the forests of Canada, meaning that once a fire starts in these areas, it is incredibly difficult to stop it. This could be due to factors such as lack of infrastructure (low accessibility) and high fuel loads, which should be taken into account in future studies. Values close to 1 mean that very rapid suppression is possible in these pixels. To explore wildfire adaptation and mitigation options in boreal forests, we artificially improved (increased) suppression efficiency across the boreal zone. To accomplish this, two adaptation scenarios were considered, which showed the effect of improving suppression efficiency in identified hotspot areas. In the first scenario, we

assumed an extreme increase in suppression efficiency, where all pixels with suppression efficiency < 0.5 were set to 0.5 (i.e., probability of fire extinguishment within 24 h). In the second scenario, all pixels with suppression efficiency < 0.2 were set to 0.2 (i.e., probability of fire extinguishment within 4 days).

Calibrated suppression efficiency values from FLAM under RCP 8.5 are shown in Figure 12 (top image). Red and orange pixels indicate areas that are unlikely to be extinguished within several days or weeks; yellow pixels indicate areas where fires are likely to be extinguished within one day; and light and dark blue pixels indicate areas where fires are likely to be extinguished in less than one day. Large areas, particularly in Siberian Russia and central Canada, are susceptible to multi-day fires. Improving suppression efficiency to within 4 days and 24 h, as shown in Figure 12 (right images), has an outstanding impact on fire spread and burned area.

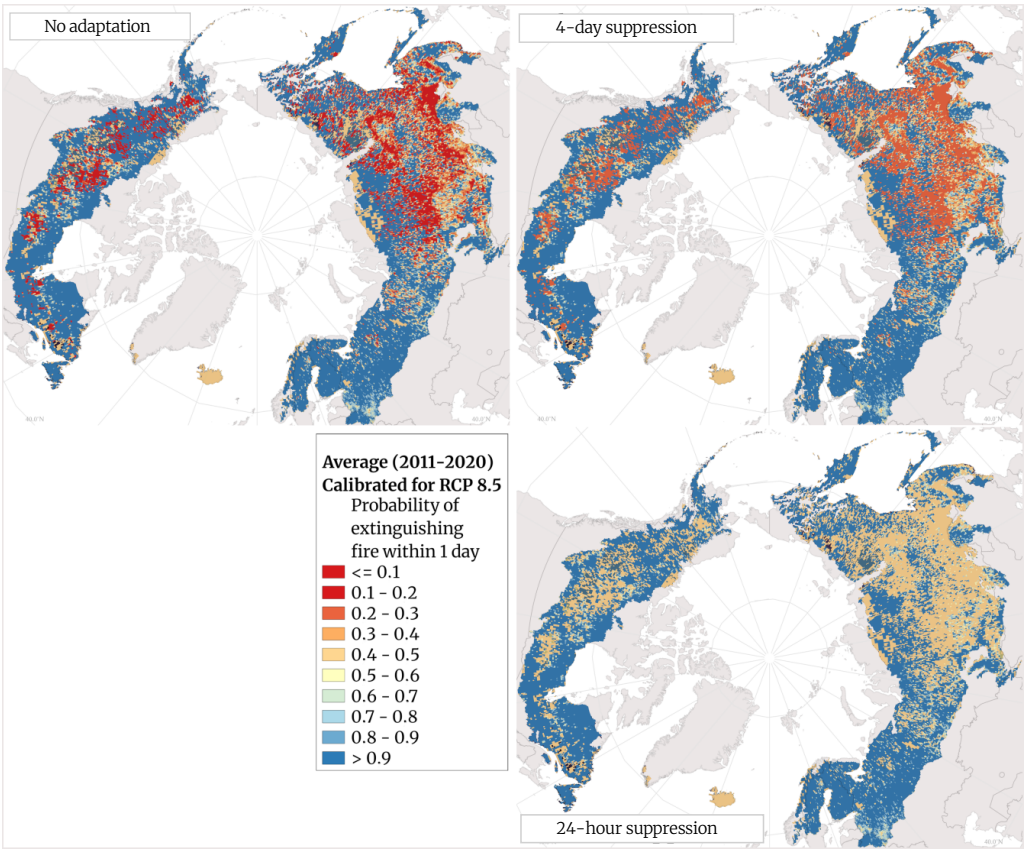

Figure 12. Suppression efficiency in the boreal forest modeled by FLAM under RCP 8.5: no adaptation scenario vs. 24 h and 4-day adaptation scenarios, 0.5 degree resolution.

Even under the worst case climate change scenario (RCP 8.5), our study shows that targeted intervention in wildfire hotspots has a drastic impact on burned area projections (Figure 13). Implementing adaptation strategies, such as improving suppression efficiency in areas like Siberian Russia and central Canada, almost halves the projected annual burned area by the end of the century if suppression is guaranteed within 4 days (threshold $q_a = 0.2$ in Equation (1)), and reduces it by nearly 5 times in the case that all fires are suppressed within 24 h (threshold $q_a = 0.5$ in Equation (1)). This can be seen by comparing the yearly burned area average across the entire future period (2021–2099) in RCP 8.5 with no adaptation with the yearly average burned area on the two adaptation scenarios (see Figure 13). To show the trends of burned area predictions over time, we used quadratic polynomial fitting for each of the scenarios. Technically, the trend line minimizes the sum of the residuals, i.e., the differences between the observations and the fits by quadratic

function. The discrepancy between the scenarios highlights the importance of management in hotspots, such as regions with low suppression efficiency.

In the no adaptation scenario, the average yearly burned area is 15.39 MHa, as compared to 7.91 MHa and 3.2 MHa in the 4-day and 24 h suppression scenarios, respectively. The potential burned forest area is therefore reduced by 48.6% and 79.2%, respectively, in the two adaptation scenarios. Despite the fact that increasing suppression efficiency at the hotspots as modelled here could be costly and time-consuming, we see that the effects of such adaptation options would be most important towards the end of the century facing more climate extremes, as suggested by RCP scenarios.

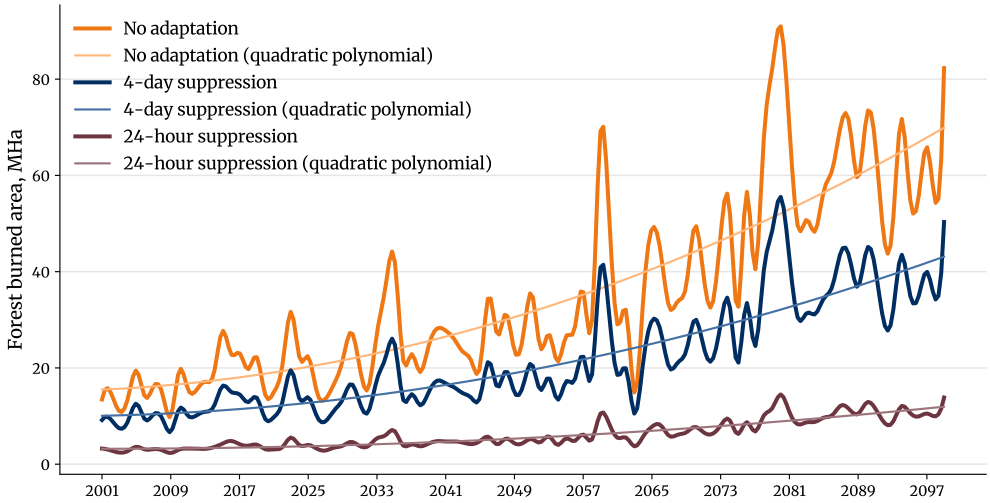

Figure 13. Burned area [MHa] (2011–2099) in the boreal forest modeled by FLAM under RCP 8.5 with no adaptation and two suppression scenarios, including quadratic polynomial trends.

4. Discussion

Weather is a key driver of wildfires, especially temperature and precipitation; hot, dry areas are susceptible to both fire ignition and spread. Therefore, climate change is certain to have a significant impact on future wildfire events, burned areas, and associated emissions. As one progresses through the RCPs from least (2.6) to most (8.5) extreme over time, it is clear that the largest changes and impacts can be expected under RCP 8.5 by the end of the century. Impacts are, however, likely to be felt as early as the period 2041–2060.

Rising temperatures are predicted under all RCPs with the projections from CMIP5 (Figure 9). While there is uncertainty about exactly how much and where temperatures will rise, it is clear that they will rise to some extent. Of concern in this regard is the expectation of warming temperatures especially in the northern parts of the boreal zone, which could not only release large amounts of greenhouse gases, but could result in reduced water stores (from melting snow and ice deposits), longer growing seasons, and northward vegetation migration. These, in turn, could result in more fuel available for burning and longer fire seasons.

Projected changes in precipitation are less certain than those predicted for temperature, where—despite the region, scenario, or model used—there is consensus that temperatures will generally rise. With precipitation, it is not easy to say that the boreal zone as a whole will experience one change; there is higher spatial variability to the changes as compared to temperature. There is less consistency between scenarios on what changes will occur where, and different modeled data could result in different precipitation values. Further, this study was not equipped to predict the form in which precipitation will occur (e.g., snow, rain, etc.) nor the changes in its form, which could have drastic impacts on vegetation growth, snowpack, and water tables—all of which have an influence on fire ignition and spread. Therefore, the conclusions drawn below must be interpreted with this limitation in mind.

Based on the modeled data used in this study, precipitation is likely to increase across more of the boreal zone by the end of the century than areas which will likely see decreases, as illustrated by the delta maps (Figure 10). Although the form, timing, and intensity of precipitation events are not included in the illustrations, the latter two are considered in the lower-resolution daily input data by FLAM (Table 1). The timing of precipitation events is important, as it influences not just vegetation growth, death, and decay, but also interacts with temperature, wind, and relative humidity to impact fuel moisture and the resultant wildfire risk (Figure 4). In light of this, one useful takeaway from the visualized precipitation changes is that they are most useful when used in conjunction with other variables, such as fuel, and most importantly, temperature change. Areas which are expected to experience both increased temperatures and either increased spring/decreased summer and autumn precipitation, or overall decreased precipitation, are likely to be most susceptible to wildfires assuming no interventions.

There is uncertainty generated by the RCP scenarios in how burned areas will evolve, particularly evident in the calibration period. Here, FLAM output aimed to reproduce the average burned areas of the historical period, which varied significantly from year to year across scenarios (Figure 8a). However, it was possible to select a modeled RCP scenario closest to FireCCI51 burned area data for each year (a so-called "best-fit scenario") (Figure 8b). While no single scenario produced a perfect fit to observations, by considering multiple scenarios, at least one of the scenarios closely captured observed values per year. The "best fit" line showed high correlation with FireCCI51 data (Table 3). Similarly, the upper and lower bounds of each prediction captured past and present conditions, lending credibility to our model's ability to capture future conditions with similar confidence. This highlights the importance of utilizing multiple potential futures/scenarios when looking at climate change impacts as well as illustrates the ability of FLAM to capture inter-annual variability provided by the FireCCI51 dataset. We cannot trust in one singular future, but we can trust that consideration of multiple futures will yield trustworthy results, especially where multiple futures result in similar or overlapping outputs (e.g., where more than one scenario identifies an area as likely to experience a fire, this can be assumed to be a hotspot or area of interest).

The compounding impacts of rising temperatures and changes in precipitation are evident in the projected burned areas from FLAM under the four RCP scenarios (see Figure 11). Maintaining current or slightly warmer temperatures such as under RCP 2.6 will still result in a slight increase in burned area (forest and total), but overall burned area is expected to be in line with current burning conditions. One should note that though temperatures are projected to increase less in RCP 6.0 compared to RCP 4.5 (Figure 9), due to lower precipitation projected in RCP 6.0 (Figure 10), FLAM projected higher burned areas under RCP 6.0 than in RCP 4.5 (Table 4). In a worst-case scenario, such as RCP 8.5, burned forest area is projected to more than triple by the end of the century without intervention. This result confirms the outcomes of previous studies on the assessment of the severity of fire weather conditions towards the end of the century, particularly in Canada and Central Russia [26,27].

Even the worst-case condition, however, can be improved by considering targeted intervention strategies such as mitigation and forest adaptation efforts in identified hotspot areas. FLAM is able to model hotspots in terms of suppression efficiency based on the historical information. These maps (Figure 12) provide important information and the possibility of modeling adaptation options. Increasing suppression efficiency to extinguish a fire within 24 h or within 4 days has considerable impacts on future burned areas modeled by FLAM (Figure 13). Future research should focus on the variables influencing the current suppression efficiency values in the hotspots, such as accessibility, infrastructure, urban interface, etc.

Of further interest is the risk which forests face at the hands of wildfires. Forests are the vegetation class most at risk of burning, with needleleaf decidious forests the most susceptible based on our results (Figure 5 and Table 2). Additional analysis would be

necessary to understand why forests are the class with the highest probability of burning and to deduce if certain forest types are more susceptible to burning, if they simply comprise a larger percentage of overall forests, or if they are more likely to burn due to external factors (e.g., proximity to agricultural fields, urbanized and developed areas, etc.).

In addition, there is a need to explore the influence of forest and vegetation type, national governance and management, adaptation options on wildfire ignitions, occurrence, spread, and projected burned areas. Research should consider monthly and other seasonal trends in wildfires and how the fire season (timing and length) may evolve under changing conditions. There is a particular need to assess the carbon emissions associated with boreal wildfires.

Finally, the results of this study are limited by its focus on assessing the impacts of climate change on wildfires. Non-climatic variables, such as population and vegetation, as well as lightning, were kept static to form a "what if" condition to isolate climate change impacts on wildfire dynamics and burned area. This study showed that climate change (changes in temperature and precipitation) will play a significant role in wildfire ignition and spread, assuming a business-as-usual scenario. Further work should be carried out to assess how results would change in conjunction with other changing variables (e.g., growing/shrinking populations, changing wildland urban interface, change in land cover and vegetation types, etc.), such as with a coupled model approach.

5. Conclusions

In this study, we conducted an analysis of future climate conditions in the boreal zone and their impact on potential burned area in both the boreal zone and boreal forests. Our model showed an increase in burned area across all RCPs and predicted extreme events, especially towards the end of the century. During calibration with the FireCCI51 data, FLAM was forced to capture average burned areas in 2011–2020. The inter-annual variability with respect to burned areas in the historical period across RCPs showed uncertainty generated by climate projections even within one model (HadGEM2). Nevertheless, the best-fit run, consisting of the selected RCPs closest to the observations for each year, showed a high Pearson's correlation, at 0.95. Notably, FLAM was able to capture large fires in the historical period.

We produced maps of fire hotspots, where fire risk is high and suppression efficiency could be improved with the highest impact on burned area. Two scenarios of improved response times were produced, which showed that stopping a fire within 4 days or within 24 h could reduce the average burned forest area by 48.6% and 79.2%, respectively, of the burned area sums over the future period (2021–2099) without adaptation. Although more research is needed to assess the costs and timing of such adaptations, their impact is most significant toward the end of the century, when the RCPs predict climate extremes. The hotspots and impacts of climate change on wildfires produced in this study provide important insight into wildfire dynamics in boreal forests, especially when considering overlap of hotspots between scenarios.

Author Contributions: Conceptualization, A.K. and F.K.; methodology, A.K. and S.C.; software, A.K., S.C. and P.K.; validation, A.K., S.C. and J.S.P.; formal analysis, A.K., S.C., C.M.V. and J.S.P.; investigation, A.K., S.C., C.M.V. and P.K.; resources, F.K.; data curation, A.K., P.K., S.C., J.S.P. and C.M.V.; writing—original draft preparation, S.C., A.K. and P.K.; writing—review and editing, S.C., A.K., P.K., J.S.P., C.M.V. and F.K.; visualization, P.K., A.K. and S.C.; supervision, F.K. and A.K.; project administration, A.K. and F.K.; funding acquisition, F.K. and A.K. All authors have read and agreed to the published version of the manuscript.

Funding: This research was funded by the project "Integrated Future Wildfire Hot Spot Mapping for Austria (Austria Fire Futures)" number C265157, funded by the Climate and Energy Fund and carried out within the framework of the Austrian Climate Research Program (ACRP).

Institutional Review Board Statement: Not applicable.

Informed Consent Statement: Not applicable.

Data Availability Statement: Data are contained within the article.

Acknowledgments: We would like to acknowledge the International Boreal Forest Research Association (IBFRA), www.ibfra.org (accessed on 21 February 2024) and the COST Action (grant no. CA18135) "Fire in the Earth System: Science & Society" (FireLinks), supported by COST (European Cooperation in Science and Technology).

Conflicts of Interest: The authors declare no conflicts of interest. The funders had no role in the design of the study; in the collection, analyses, or interpretation of data; in the writing of the manuscript; or in the decision to publish the results.

References

1. Apps, M.; Kurz, W.; Luxmoore, R.; Nilsson, L.; Sedjo, R.; Schmidt, R.; Simpson, L.; Vinson, T. Boreal forests and tundra. *Water Air Soil Pollut.* **1993**, *70*, 39–53. [CrossRef]
2. Högberg, P.; Ceder, L.; Astrup, R.; Binkley, D.; Dalsgaard, L.; Egnell, G.; Filipchuk, A.; Genet, H.; Ilintsev, A.; Kurz, W.; et al. *Sustainable Boreal Forest Management Challenges and Opportunities for Climate Change Mitigation*; Swedish Forest Agency: Jönköping, Sweden, 2021.
3. Burrell, A.L.; Sun, Q.; Baxter, R.; Kukavskaya, E.A.; Zhila, S.; Shestakova, T.; Rogers, B.M.; Kaduk, J.; Barrett, K. Climate change, fire return intervals and the growing risk of permanent forest loss in boreal Eurasia. *Sci. Total Environ.* **2022**, *831*, 154885. [CrossRef] [PubMed]
4. Flannigan, M.; Cantin, A.S.; de Groot, W.J.; Wotton, M.; Newbery, A.; Gowman, L.M. Global wildland fire season severity in the 21st century. *For. Ecol. Manag.* **2013**, *294*, 54–61. [CrossRef]
5. Furyaev, V.V. *Pozharoustoychivost Sosnovykh Lesov*; Nauka: Moscow, Russia, 2005.
6. Minsley, B.J.; Pastick, N.J.; Wylie, B.K.; Brown, D.R.; Andy Kass, M. Evidence for nonuniform permafrost degradation after fire in boreal landscapes. *J. Geophys. Res. Earth Surf.* **2016**, *121*, 320–335. [CrossRef]
7. Johnstone, J.F.; Rupp, T.S.; Olson, M.; Verbyla, D. Modeling impacts of fire severity on successional trajectories and future fire behavior in Alaskan boreal forests. *Landsc. Ecol.* **2011**, *26*, 487–500. [CrossRef]
8. Li, X.Y.; Jin, H.J.; Wang, H.W.; Marchenko, S.S.; Shan, W.; Luo, D.L.; He, R.X.; Spektor, V.; Huang, Y.D.; Li, X.Y.; et al. Influences of forest fires on the permafrost environment: A review. *Adv. Clim. Chang. Res.* **2021**, *12*, 48–65. [CrossRef]
9. Triviño, M.; Potterf, M.; Tijerín, J.; Ruiz-Benito, P.; Burgas, D.; Eyvindson, K.; Blattert, C.; Mönkkönen, M.; Duflot, R. Enhancing Resilience of Boreal Forests Through Management Under Global Change: A Review. *Curr. Landsc. Ecol. Rep.* **2023**, *8*, 103–118. [CrossRef]
10. Li, T.; Cui, L.; Liu, L.; Chen, Y.; Liu, H.; Song, X.; Xu, Z. Advances in the study of global forest wildfires. *J. Soils Sediments* **2023**, *23*, 2654–2668. [CrossRef]
11. Chuvieco, E.; Pettinari, M.L.; Lizundia-Loiola, J.; Storm, T.; Parellada, M.P. *ESA Fire Climate Change Initiative (Fire_cci): MODIS Fire_cci Burned Area Pixel product, Version 5.1 (3.1)*; Centre for Environmental Data Analysis (CEDA): Chilton, UK, 2018.
12. Chuvieco, E.; Lizundia-Loiola, J.; Pettinari, M.L.; Ramo, R.; Padilla, M.; Tansey, K.; Mouillot, F.; Laurent, P.; Storm, T.; Heil, A.; et al. Generation and analysis of a new global burned area product based on MODIS 250 m reflectance bands and thermal anomalies. *Earth Syst. Sci. Data* **2018**, *10*, 2015–2031. [CrossRef]
13. Phillips, C.A.; Rogers, B.M.; Elder, M.; Cooperdock, S.; Moubarak, M.; Randerson, J.T.; Frumhoff, P.C. Escalating carbon emissions from North American boreal forest wildfires and the climate mitigation potential of fire management. *Sci. Adv.* **2022**, *8*, eabl7161. [CrossRef]
14. Hu, Y.; Yue, X.; Tian, C. Climatic drivers of the Canadian wildfire episode in 2023. *Atmos. Ocean. Sci. Lett.* **2024**, 100483. [CrossRef]
15. Cimdins, R.; Krasovskiy, A.; Kraxner, F. Regional Variability and Driving Forces behind Forest Fires in Sweden. *Remote Sens.* **2022**, *14*, 5826. [CrossRef]
16. Kharuk, V.I.; Dvinskaya, M.L.; Im, S.T.; Golyukov, A.S.; Smith, K.T. Wildfires in the Siberian Arctic. *Fire* **2022**, *5*, 106. [CrossRef]
17. Bradshaw, C.J.; Warkentin, I.G. Global estimates of boreal forest carbon stocks and flux. *Glob. Planet. Chang.* **2015**, *128*, 24–30. [CrossRef]
18. Ameray, A.; Bergeron, Y.; Valeria, O.; Montoro Girona, M.; Cavard, X. Forest carbon management: A review of silvicultural practices and management strategies across boreal, temperate and tropical forests. *Curr. For. Rep.* **2021**, *7*, 245–266. [CrossRef]
19. Gauthier, S.; Kuuluvainen, T.; Macdonald, S.E.; Shorohova, E.; Shvidenko, A.; Bélisle, A.C.; Vaillancourt, M.A.; Leduc, A.; Grosbois, G.; Bergeron, Y.; et al. Ecosystem management of the boreal forest in the era of global change. In *Boreal Forests in the Face of Climate Change: Sustainable Management*; Springer: Berlin/Heidelberg, Germany, 2023; pp. 3–49.
20. Dieleman, C.M.; Rogers, B.M.; Potter, S.; Veraverbeke, S.; Johnstone, J.F.; Laflamme, J.; Solvik, K.; Walker, X.J.; Mack, M.C.; Turetsky, M.R. Wildfire combustion and carbon stocks in the southern Canadian boreal forest: Implications for a warming world. *Glob. Chang. Biol.* **2020**, *26*, 6062–6079. [CrossRef] [PubMed]
21. Parisien, M.A.; Barber, Q.E.; Hirsch, K.G.; Stockdale, C.A.; Erni, S.; Wang, X.; Arseneault, D.; Parks, S.A. Fire deficit increases wildfire risk for many communities in the Canadian boreal forest. *Nat. Commun.* **2020**, *11*, 2121. [CrossRef] [PubMed]
22. Zheng, B.; Ciais, P.; Chevallier, F.; Yang, H.; Canadell, J.G.; Chen, Y.; van der Velde, I.R.; Aben, I.; Chuvieco, E.; Davis, S.J.; et al. Record-high CO_2 emissions from boreal fires in 2021. *Science* **2023**, *379*, 912–917. [CrossRef] [PubMed]

23. Rantanen, M.; Karpechko, A.Y.; Lipponen, A.; Nordling, K.; Hyvärinen, O.; Ruosteenoja, K.; Vihma, T.; Laaksonen, A. The Arctic has warmed nearly four times faster than the globe since 1979. *Commun. Earth Environ.* **2022**, *3*, 168. [CrossRef]
24. Flannigan, M.D.; Amiro, B.D.; Logan, K.A.; Stocks, B.J.; Wotton, B.M. Forest fires and climate change in the 21 st century. *Mitig. Adapt. Strateg. Glob. Chang.* **2006**, *11*, 847–859. [CrossRef]
25. Kharuk, V.I.; Ponomarev, E.I.; Ivanova, G.A.; Dvinskaya, M.L.; Coogan, S.C.; Flannigan, M.D. Wildfires in the Siberian taiga. *Ambio* **2021**, *50*, 1953–1974. [CrossRef]
26. Wang, X.; Studens, K.; Parisien, M.A.; Taylor, S.W.; Candau, J.N.; Boulanger, Y.; Flannigan, M.D. Projected changes in fire size from daily spread potential in Canada over the 21st century. *Environ. Res. Lett.* **2020**, *15*, 104048. [CrossRef]
27. de Groot, W.J.; Flannigan, M.D.; Cantin, A.S. Climate change impacts on future boreal fire regimes. *For. Ecol. Manag.* **2013**, *294*, 35–44. [CrossRef]
28. Shvidenko, A.; Shchepashchenko, D.; Vaganov, E.; Sukhinin, A.; Maksyutov, S.S.; McCallum, I.; Lakyda, I. Impact of wildfire in Russia between 1998–2010 on ecosystems and the global carbon budget. *Dokl. Earth Sci.* **2011**, *441*, 1678–1682. [CrossRef]
29. Burton, C.; Lampe, S.; Kelley, D.; Thiery, W.; Hantson, S.; Christidis, N.; Gudmundsson, L.; Forrest, M.; Burke, E.; Chang, J.; et al. Global burned area increasingly explained by climate change. *Res. Sq.* 2023, *in press*. [CrossRef]
30. Arora, V.K.; Boer, G.J. Fire as an interactive component of dynamic vegetation models. *J. Geophys. Res. Biogeosci.* **2005**, *110*, G02008. [CrossRef]
31. Wagner, C.E.V.; Pickett, T.L. *Equations and FORTRAN Program for the Canadian Forest Fire Weather Index System*; Forestry Technical Report; Canadian Forestry Service, Petawawa National Forestry Institute: Chalk River, ON, Canada, 1985; Volume 33, p. 18. Available online: http://cfs.nrcan.gc.ca/publications?id=19973 (accessed on 21 February 2024) .
32. Khabarov, N.; Krasovskii, A.; Obersteiner, M.; Swart, R.; Dosio, A.; San-Miguel-Ayanz, J.; Durrant, T.; Camia, A.; Migliavacca, M. Forest fires and adaptation options in Europe. *Reg. Environ. Chang.* **2016**, *16*, 21–30. [CrossRef]
33. Krasovskii, A.; Khabarov, N.; Migliavacca, M.; Kraxner, F.; Obersteiner, M. Regional aspects of modelling burned areas in Europe. *Int. J. Wildland Fire* **2016**, *25*, 811–818. [CrossRef]
34. Jo, H.W.; Krasovskiy, A.; Hong, M.; Corning, S.; Kim, W.; Kraxner, F.; Lee, W.K. Modeling Historical and Future Forest Fires in South Korea: The FLAM Optimization Approach. *Remote Sens.* **2023**, *15*, 1446. [CrossRef]
35. Krasovskii, A.; Khabarov, N.; Pirker, J.; Kraxner, F.; Yowargana, P.; Schepaschenko, D.; Obersteiner, M. Modeling burned areas in Indonesia: The FLAM approach. *Forests* **2018**, *9*, 437. [CrossRef]
36. Chu, T.; Guo, X. Remote sensing techniques in monitoring post-fire effects and patterns of forest recovery in boreal forest regions: A review. *Remote Sens.* **2013**, *6*, 470–520. [CrossRef]
37. Xu, W.; Wooster, M.J. Sentinel-3 SLSTR active fire (AF) detection and FRP daytime product-Algorithm description and global intercomparison to MODIS, VIIRS and landsat AF data. *Sci. Remote Sens.* **2023**, *7*, 100087. [CrossRef]
38. Pessôa, A.C.M.; Anderson, L.O.; Carvalho, N.S.; Campanharo, W.A.; Junior, C.H.S.; Rosan, T.M.; Reis, J.B.; Pereira, F.R.; Assis, M.; Jacon, A.D.; et al. Intercomparison of burned area products and its implication for carbon emission estimations in the amazon. *Remote Sens.* **2020**, *12*, 3864. [CrossRef]
39. Dutta, R.; Aryal, J.; Das, A.; Kirkpatrick, J.B. Deep cognitive imaging systems enable estimation of continental-scale fire incidence from climate data. *Sci. Rep.* **2013**, *3*, 3188. [CrossRef] [PubMed]
40. Giglio, L.; Randerson, J.T.; Van Der Werf, G.R. Analysis of daily, monthly, and annual burned area using the fourth-generation global fire emissions database (GFED4). *J. Geophys. Res. Biogeosci.* **2013**, *118*, 317–328. [CrossRef]
41. Lizundia-Loiola, J.; Otón, G.; Ramo, R.; Chuvieco, E. A spatio-temporal active-fire clustering approach for global burned area mapping at 250 m from MODIS data. *Remote Sens. Environ.* **2020**, *236*, 111493. [CrossRef]
42. Hantson, S.; Arneth, A.; Harrison, S.P.; Kelley, D.I.; Prentice, I.C.; Rabin, S.S.; Archibald, S.; Mouillot, F.; Arnold, S.R.; Artaxo, P.; et al. The status and challenge of global fire modelling. *Biogeosciences* **2016**, *13*, 3359–3375. [CrossRef]
43. Chen, Y.; Morton, D.C.; Jin, Y.; Collatz, G.J.; Kasibhatla, P.S.; van der Werf, G.R.; DeFries, R.S.; Randerson, J.T. Long-term trends and interannual variability of forest, savanna and agricultural fires in South America. *Carbon Manag.* **2013**, *4*, 617–638. [CrossRef]
44. Andela, N.; Morton, D.C.; Giglio, L.; Chen, Y.; van der Werf, G.R.; Kasibhatla, P.S.; DeFries, R.S.; Collatz, G.; Hantson, S.; Kloster, S.; et al. A human-driven decline in global burned area. *Science* **2017**, *356*, 1356–1362. [CrossRef]
45. Yulianti, N.; Hayasaka, H.; Sepriando, A. Recent trends of fire occurrence in Sumatra (analysis using MODIS hotspot data): A comparison with fire occurrence in Kalimantan. *Open J. For.* **2013**, *3*, 129–137. [CrossRef]
46. Van Vuuren, D.P.; Edmonds, J.; Kainuma, M.; Riahi, K.; Thomson, A.; Hibbard, K.; Hurtt, G.C.; Kram, T.; Krey, V.; Lamarque, J.F.; et al. The representative concentration pathways: An overview. *Clim. Chang.* **2011**, *109*, 5–31. [CrossRef]
47. Riahi, K.; Rao, S.; Krey, V.; Cho, C.; Chirkov, V.; Fischer, G.; Kindermann, G.; Nakicenovic, N.; Rafaj, P. RCP 8.5—A scenario of comparatively high greenhouse gas emissions. *Clim. Chang.* **2011**, *109*, 33–57. [CrossRef]
48. Brandt, J.P.; Flannigan, M.; Maynard, D.; Thompson, I.; Volney, W. An introduction to Canada's boreal zone: Ecosystem processes, health, sustainability, and environmental issues. *Environ. Rev.* **2013**, *21*, 207–226. [CrossRef]
49. Seidl, R.; Fortin, M.J.; Honkaniemi, J.; Lucash, M. Modeling Natural Disturbances in Boreal Forests. In *Boreal Forests in the Face of Climate Change: Sustainable Management*; Springer: Berlin/Heidelberg, Germany, 2023; pp. 591–612.
50. Kasischke, E.S.; Verbyla, D.L.; Rupp, T.S.; McGuire, A.D.; Murphy, K.A.; Jandt, R.; Barnes, J.L.; Hoy, E.E.; Duffy, P.A.; Calef, M.; et al. Alaska's changing fire regime—Implications for the vulnerability of its boreal forests. *Can. J. For. Res.* **2010**, *40*, 1313–1324. [CrossRef]

51. Achard, F.; Eva, H.D.; Mollicone, D.; Beuchle, R. The effect of climate anomalies and human ignition factor on wildfires in Russian boreal forests. *Philos. Trans. R. Soc. B Biol. Sci.* **2008**, *363*, 2329–2337. [CrossRef]
52. The International Boreal Forest Research Association (IBFRA). About Boreal Forests. Available online: http://ibfra.org/about-boreal-forests/ (accessed on 14 February 2024).
53. Williams, A.P.; Abatzoglou, J. Recent Advances and Remaining Uncertainties in Resolving Past and Future Climate Effects on Global Fire Activity. *Curr. Clim. Chang. Rep.* **2016**, *2*, 1–14. [CrossRef]
54. An, H.; Gan, J.; Cho, S.J. Assessing climate change impacts on wildfire risk in the United States. *Forests* **2015**, *6*, 3197–3211. [CrossRef]
55. Chen, Y.R.D.S.J. Future increases in Arctic lightning and fire risk for permafrost carbon. *Nat. Clim. Chang.* **2021**, *11*, 404–410. [CrossRef]
56. Frieler, K.; Lange, S.; Piontek, F.; Reyer, C.P.; Schewe, J.; Warszawski, L.; Zhao, F.; Chini, L.; Denvil, S.; Emanuel, K.; et al. Assessing the impacts of 1.5 C global warming–simulation protocol of the Inter-Sectoral Impact Model Intercomparison Project (ISIMIP2b). *Geosci. Model Dev.* **2017**, *10*, 4321–4345. [CrossRef]
57. Collins, W.; Bellouin, N.; Doutriaux-Boucher, M.; Gedney, N.; Halloran, P.; Hinton, T.; Hughes, J.; Jones, C.; Joshi, M.; Liddicoat, S.; et al. Development and evaluation of an Earth-System model–HadGEM2. *Geosci. Model Dev.* **2011**, *4*, 1051–1075. [CrossRef]
58. Karger, D.N.; Conrad, O.; Böhner, J.; Kawohl, T.; Kreft, H.; Soria-Auza, R.W.; Zimmermann, N.E.; Linder, H.P.; Kessler, M. Climatologies at high resolution for the earth's land surface areas. *Sci. Data* **2017**, *4*, 1–20. [CrossRef] [PubMed]
59. Center for International Earth Science Information Network (CIESIN), Columbia University. *Documentation for the Gridded Population of the World, Version 4 (GPWv4), Revision 11 Data Sets*; NASA Socioeconomic Data and Applications Center (SEDAC): Palisades, NY, USA, 2018. [CrossRef]
60. Cecil, D. *LIS/OTD 0.5 Degree High Resolution Annual Climatology (HRAC)*; NASA Global Hydrology Resource Center DAAC: Huntsville, AL, USA, 2006.
61. Kindermann, G.; McCallum, I.; Fritz, S.; Obersteiner, M. A global forest growing stock, biomass and carbon map based on FAO statistics. *Silva Fenn.* **2008**, *42*, 387–396. [CrossRef]